Adding a third dimension to operando spectroscopy: a combined UV-Vis, Raman and XAFS setup to study heterogeneous catalysts under working conditions†

Andrew M. Beale,[a] Ad M. J. van der Eerden,[a] Kaisa Kervinen,[a] Mark A. Newton[b] and Bert M. Weckhuysen*[a]

The potential of combined operando UV-Vis/Raman/XAFS has been explored by studying the active site and deactivation mechanism of silica- and alumina-supported molybdenum oxide catalysts under propane dehydrogenation conditions.

Ideally scientists would like to take real-time spectra inside a catalytic reactor when a catalytic process is operating, giving them detailed insight into the working principles of the catalytic material.[1] On this basis, it would then be possible to improve upon existing catalyst formulations or design completely new ones, which are more active and/or selective. Such rational catalyst design is still a dream since the experimental tools available to study the active catalyst do not yet provide sufficient insight. In this respect, it is advantageous to look on catalytic systems from different perspectives by making use of multiple characterisation techniques. In recent years, many attempts have been made to combine multiple spectroscopic techniques into one experimental set-up. The following combinations of two spectroscopic techniques have been recently reported for studying heterogeneous catalysts in action: EPR/UV-Vis, NMR/UV-Vis, XAFS/IR, UV-Vis/Raman and IR/UV-Vis.[2–7]

Here, we describe a newly developed and powerful operando set-up to measure combined energy-dispersive (ED)-XAFS, UV-Vis and Raman to study a working catalytic solid. To our best knowledge, this is the first device which couples three spectroscopic techniques in one reactor, focuses on the same spot of a metal oxide catalyst under true reaction conditions and is capable of delivering sub second time resolution. A scheme of the set-up is given in Fig. 1. Further details are given in the ESI.†

The operando device developed is widely applicable in the field of heterogeneous catalysis and its potential has been explored for the dehydrogenation of propane (5% in He) over supported Mo catalysts which have shown potential for alkane activation.[8,9] We have studied 13 wt% Mo/Al_2O_3 and Mo/SiO_2 catalysts during successive propane dehydrogenation cycles at 550 °C. The three techniques are sensitive to changes in the oxidation/coordination states of Mo allowing us to obtain complementary information on the catalysts behaviour during dehydrogenation and regeneration. The set-up allows us to discriminate between the dynamics of both catalysts under reaction conditions and to identify the possible active site and deactivation pathways. Also the complementary

aspects of this setup are demonstrated by showing how the catalyst undergoes changes which cannot be followed using one of the techniques alone and how it is possible to obtain quantitative Raman information without the use of an internal standard.

Fig. 2 shows data collected using the three techniques during the first propane dehydrogenation cycle (PC1) for Mo/SiO_2. The initial features observed in the spectra included a distinct 1s–4d pre-edge feature at 20002 eV in the ED-XANES, a strong LMCT band at *ca.* 350 nm in the UV-Vis and Raman bands at 992 ($\nu Mo=O$), 820 and 664 ($\nu Mo–O–Mo$), 335 ($\delta Mo–O–Mo$) and 281 ($\delta Mo=O$) cm^{-1} respectively.[10] All are consistent with previous observations for supported molybdenum catalysts in which Mo^{6+} species are present as a mixture of distorted tetrahedral and octahedral environments (MoO_3 aggregates form due to a poor interaction with the silica support).[11,12] These features however were observed to quickly diminish during the subsequent propane dehydrogenation step. Most notably the bands corresponding to the MoO_3 phase as well as a band at 1350 cm^{-1} (the BN internal standard) and the high baseline at higher wavenumbers caused by fluorescence from the catalyst had disappeared after only 10 min. This corresponded with a levelling off of the UV-Vis spectra and an overall decrease in the diffuse reflectance from the sample. These changes suggested a darkening of the catalyst which would occur if the Mo was being reduced or if coke was to form. Indeed the changes in the ED-XANES data which included a decline in pre-edge peak intensity, an increase in the 1s-5p transition feature at 20022 eV and a shift in the white line from 20011 to 20010 eV which continued until the reaction ceased some 20 min later, was consistent with a reduction of some of the Mo^{6+} to Mo^{4+}. Evidence
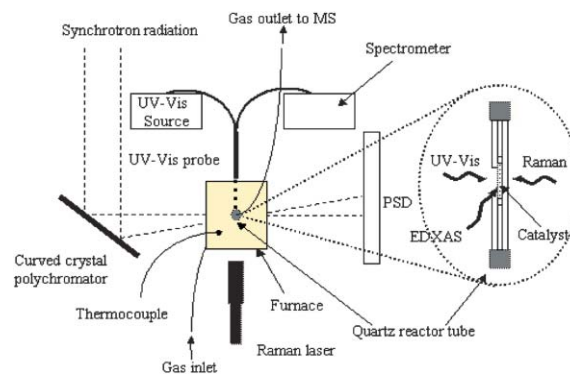

Fig. 1 Scheme of the multitechnique operando setup making use of UV-Vis, Raman and ED-XAFS. To the right is an enlarged image of the reactor cell.
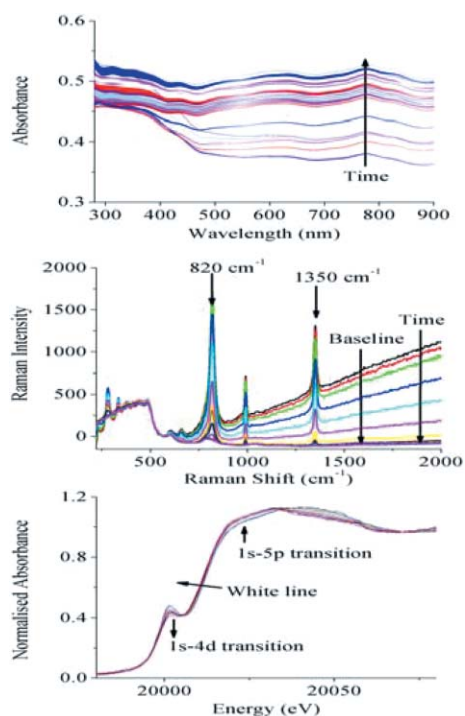
Fig. 2 Time-resolved UV-Vis (top), Raman (middle) and ED-XANES (bottom) spectra acquired during PC1 for Mo/SiO$_2$. The time between each acquisition presented is 60 s for each technique and the arrows represent progress with time.
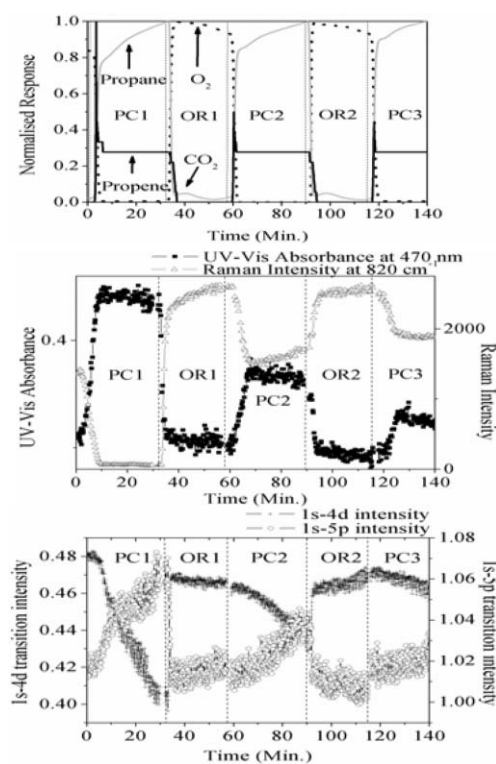

Fig. 3 Time-resolved data collected during successive propane dehydrogenation cycles (PC1–3) and oxidative regeneration cycles (OR1,2) for Mo/SiO$_2$. The dashed lines represent the reaction times at which a new cycle began.

for this reduction (shift to a shorter wavelength of the LMCT band) was not observed in the UV-Vis data which would imply that coke formation on the catalyst was the cause of the increase in UV-Vis absorbance at the beginning of the reaction.

The data described above are summarized in Fig. 3. The corresponding plots detail the changes in key features of each spectrum during dehydrogenation and regeneration. It appeared that the darkening of the catalyst at the beginning of the cycle coincided with a decline in propene production suggesting that coking caused an initial deactivation (however, no sharp Raman bands between 1200–1650 cm^{-1} due to coke were observed). After this point the catalytic performance remained constant. Upon switching the feed gas to a 5% O$_2$/He mixture for regeneration, the changes observed during PC1 were reversed (<2 min) although a large increase in the Raman signal intensity for the band at 820 cm^{-1}, a lower UV-Vis diffuse reflectance and a weaker 1s–4d transition in the ED-XANES suggested that further polymerisation of the molybdenum resulting in larger MoO$_3$ clusters occurred. However, it would appear at this stage that these clusters had reached a critical size since very little change in the Raman band intensity was observed between OR1 and OR2. CO$_2$ formation was also detected at this point which is consistent with burning of coke or else combustion of any remaining propane.

For the second (PC2) and third (PC3) propane dehydrogenation steps the initial flurry of propene production in the first minute was followed by a steady conversion and this was again accompanied by a gradual decrease in Raman intensity and UV-Vis diffuse reflectance during the first 10 min. However, unlike the first cycle the Raman bands corresponding to MoO$_3$ did not completely disappear. Furthermore, only a small reduction in the

1s–4d transition intensity was observed in the ED-XANES data suggesting that these larger MoO$_3$ clusters were difficult to reduce.

Fig. 4 shows the results for multiple dehydrogenation/ regeneration cycles for Mo/Al$_2$O$_3$. In contrast to Mo/SiO$_2$ the position of the LMCT band in the UV-Vis and strong pre-edge peak intensity in the ED-XANES data as well as an absence of any strong Raman bands is indicative of dispersed Mo^{6+} tetrahedra on the catalyst surface.[12,13] However, similar to Mo/SiO$_2$ the activity for propene production during PC1 was comparatively high and slowly declined with time (*ca.* 10 min). Furthermore, this initial high conversion could not be re-obtained in the subsequent dehydrogenation steps. During each of these steps absorption of the UV-Vis light increased in the first 5 min and was accompanied by a decrease in the Raman background fluorescence, whereas the intensity of the pre-edge peak associated with the 1s–4d transition in the ED-XANES only exhibited a small reduction with time. As with Mo/SiO$_2$, the most likely explanation for the initial changes observed in the Raman and UV-Vis data is the formation of coke on the catalyst since again no shift in the LMCT band to a higher energy and no d–d bands indicative of the presence of reduced Mo species were observed. It is likely though that the changes in the ED-XANES are due to reduction of the dispersed Mo^{6+} to Mo^{4+}. However, it appeared that reduction in the pre-peak intensity in the ED-XANES became more pronounced with each reduction cycle and never regained the full initial intensity which hinted at some changes in the catalyst sample that correlate with a decline in overall activity.
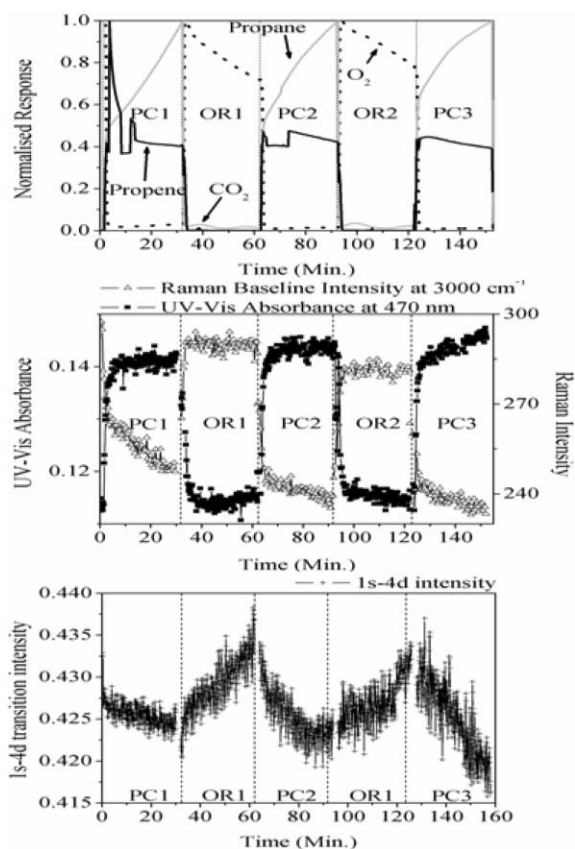
Fig. 4 Time-resolved data collected during successive propane cycles (PC1–3) and oxidative regeneration cycles (OR1,2) for Mo/Al$_2$O$_3$. The dashed lines represent the times at which a new cycle began.

In conclusion, both catalysts showed activity for propane to propene conversion, but they deactivate over time *via* two processes: an initial deactivation due to coke formation and a more permanent one as a result of bulk changes. Coke formation is a common problem affecting the activity of propane dehydrogenation catalysts[14] and this occurred more quickly on Mo/Al$_2$O$_3$ than on Mo/SiO$_2$. However, the coke is easily removed during regeneration. The changes in the ED-XANES data however were due to Mo^{6+} to Mo^{4+} reduction which is the most significant for Mo/SiO$_2$ during PC1 suggesting that the initial MoO$_3$ clusters present on this catalyst are easier to reduce than the large clusters that form later. For Mo/Al$_2$O$_3$ the dispersed species on this catalyst are also difficult to reduce and hence little change in the ED-XANES data was observed. The initial deactivation may also reflect a change in the catalytic mechanism which yields propene. Any oxygen remaining in the reactor and an unreduced/coke-free catalyst surface may favour oxidative dehydrogenation but as this is used up and coking occurs, dehydrogenation takes over. However, the propene yield was much lower at this stage and continues to decline as more coke was formed. It would therefore appear that oxidative dehydrogenation is a more efficient mechanism for producing propene on these catalysts. For Mo/SiO$_2$ the initial propene yield followed the trend PC1 > PC2 > PC3 and it appeared that clustering of the MoO$_3$ results in

irreversible catalyst deactivation. For Mo/Al$_2$O$_3$ long term deactivation may occur as a result of a reaction of the Mo with the Al$_2$O$_3$ support to form an inactive phase as suggested by the changes in the ED-XANES with time. It is possible to conclude therefore that the catalytically active part of both catalysts involves the dispersed Mo over the surface, most probably as Mo^{4+}.

In summary, we have demonstrated how a new spectroscopic tool can be used to obtain valuable information on the behaviour of a catalytic solid under reaction conditions, affording a unique insight into the origin of activity and deactivation. It would appear that the presence of Mo^{4+} species in both catalysts may be necessary for catalytic activity. However, coke formation and solid state reactions on/with the catalyst surface lead to temporary or permanent deactivation. Clearly, this operando setup is capable of providing a lot of congruous information in one experiment thereby demonstrating the potential of a new and powerful tool for studying heterogeneous catalytic processes as well as other scientific disciplines.‡

Andrew M. Beale,[a] **Ad M. J. van der Eerden,**[a] **Kaisa Kervinen,**[a] **Mark A. Newton**[b] **and Bert M. Weckhuysen***[a]
[a]*Department of Inorganic Chemistry and Catalysis, Debye Institute, Utrecht University, Sorbonnelaan 16, 3508 TC, Utrecht, The Netherlands. E-mail: b.m.weckhuysen@chem.uu.nl; Fax: +31 30 253 1027; Tel: +31 30 2537400*
[b]*The ESRF, BP 220, 38043, Grenoble, Cedex 9, France*

Notes and references

‡ We note that very recently an apparatus has been developed in parallel to ours, which integrates UV-Vis/Raman and EPR into one operando setup.[15]

1 (*a*) B. M. Weckhuysen, *Chem. Commun.*, 2002, 97; (*b*) B. M. Weckhuysen, *Phys. Chem. Chem. Phys.*, 2003, **5**, 4351.
2 A. Brückner, *Chem. Commun.*, 2001, 2122.
3 A. Brückner, *Catal. Rev. Sci. Eng.*, 2003, **45**, 97.
4 M. Hunger and W. Wang, *Chem. Commun.*, 2004, 584.
5 M. A. Newton, B. Jyoti, A. J. Dent, S. G. Fiddy and J. Evans, *Chem. Commun.*, 2004, 2382.
6 (*a*) T. A. Nijhuis, S. J. Tinnemans, T. Visser and B. M. Weckhuysen, *Phys. Chem. Chem. Phys.*, 2003, **5**, 4361; (*b*) S. J. Tinnemans, M. H. F. Kox, T. A. Nijhuis, T. Visser and B. M. Weckhuysen, *Phys. Chem. Chem. Phys.*, 2005, **7**, 211.
7 T. Bürgi, *J. Catal.*, 2005, **229**, 55.
8 M. E. Harlin, L. B. Backman, A. O. I. Krause and O. J. T. Jylha, *J. Catal.*, 1999, **183**, 300.
9 K. Chen, S. Xie, A. T. Bell and E. Iglesia, *J. Catal.*, 2001, **198**, 232.
10 L. Seguin, M. Figlarz, R. Cavagnat and J. C. Lassègues, *Spectrochim. Chemica Acta A.*, 1995, **53**, 1323.
11 C. C. Williams, J. G. Ekerdt, J. M. Jehng, F. D. Hardcastle, A. M. Turek and I. E. Wachs, *J. Phys. Chem.*, 1991, **95**, 8781.
12 C. Thomazeau, V. Martin and P. Afanasiev, *Appl. Catal. A: General*, 2000, **199**, 61.
13 C. C. Williams, J. G. Ekerdt, J. M. Jehng, F. D. Hardcastle and I. E. Wachs, *J. Phys. Chem.*, 1991, **95**, 8791.
14 T. V. Annaland, J. A. M. Kuipers and W. P. M. van Swaaij, *Catal. Today*, 2001, **66**, 427.
15 A. Brückner, *Chem. Commun.*, 2005, 1761 and personal communication.